

Quantization of the chiral soliton in medium

S.Nagai, N.Sawado,* and N.Shiiki†

*Department of Physics, Faculty of Science and Technology,
Tokyo University of Science, Noda, Chiba 278-8510, Japan*

(Dated: February 2, 2008)

Chiral solitons coupled with quarks in medium are studied based on the Wigner-Seitz approximation. The chiral quark soliton model is used to obtain the classical soliton solutions. To investigate nucleon and Δ in matter, the semi-classical quantization is performed by the cranking method. The saturation for nucleon matter and Δ matter are observed.

PACS numbers: 12.39.Fe, 12.39.Ki, 21.65.+f, 24.85.+p

I. INTRODUCTION

The study of dense nuclear matter with the internal nucleon structure is old but still a challenging subject. Especially, the approach of the topological soliton model seems interesting, because it is believed as a low energy effective model in the large N_c -limit of QCD. It was first applied for nuclear matter system in 80's by using the skyrmion centered cubic (CC) crystal by Klebanov [1]. This configuration was studied further by Wüst, Brown and Jackson to estimate the baryon density and discuss the phase transition between nuclear matter and quark matter [2]. Goldhaber and Manton found a new configuration, body centered cubic (BCC) of half-skyrmions in a higher density regime [3]. The face centered cubic (FCC) and BCC lattice were also studied by Castillejo *et al.* [4] and the phase transitions between those configurations were investigated by Kugler and Shtrikman [5]. Recently, the idea of using crystallized skyrmions to study nuclear matter was revived by Park, Min, Rho and Vento with the introduction of the Atiyah-Manton multi-soliton ansatz in a unit cell [6].

Incorporating quark degrees of freedom into each soliton makes the prediction more realistic. Achterhues, Scheid and Wilets investigated the Friedberg-Lee soliton bag model with a simple cubic lattice [7]. Due to the periodicity of the background potential, the solution of the Dirac equation has the form of the Bloch waves, $\psi_{\mathbf{k}}(\mathbf{r}) = e^{i\mathbf{k}\cdot\mathbf{r}}\phi_{\mathbf{k}}(\mathbf{r})$ where $\phi_{\mathbf{k}}$ satisfies the same periodic boundary condition as the background potential. They performed the calculation for only one direction of the crystal momenta $\mathbf{k} = k\mathbf{e}_z$ and assumed the spherically symmetric energy surface. The Bloch condition is, however, anisotropic for the nonzero \mathbf{k} and the results should be highly dependent on the approximation. The analysis of the crystal soliton model with quarks based on the Wigner-Seitz approximation has been already done. In this ansatz, a single soliton is placed on the center of a spherical unit cell. Then the lowest energy level ("bottom" of the band) for the valence quarks becomes s-state.

The appropriate boundary conditions at the cell boundary should be imposed on the quark wave functions as well as the chiral fields. This simple treatment sheds light on the nucleon structure in nuclear medium. Soliton matter within this approximation have been extensively studied by using various nucleon models such as the chiral quark-meson type model [8, 9, 10, 11], Friedberg-Lee soliton bag model [11, 12, 13, 14], the Skyrme model [15]. The non-zero dispersion of the lowest band [11] and the quark-meson coupling [14] were also examined within this approximation.

The chiral quark soliton model (CQSM) can be interpreted as the soliton bag model including not only valence quarks but also the vacuum sea quark polarization effects explicitly [16, 17, 18]. The model provides correct observables of a nucleon such as mass, electromagnetic value, spin carried by quarks, parton distributions and octet, decuplet $SU(3)$ baryon spectra [19]. Remarkably this model predicted the exotic quark bound state, pentaquark Θ^+ [20] which was successfully observed in experiments [21].

Amore and De Pace studied soliton matter in the CQSM using the Wigner-Seitz approximation and observed the nuclear saturation [22]. They examined the soliton solutions with three different boundary conditions imposed on the quark wave function. However the obtained saturation density was higher than the experimental value and they concluded that such discrepancy is originated in the approximate treatment of the sea quark contribution [23]. Thus we treat the vacuum polarization exactly in the manner originally proposed by Kahana and Ripka [24] and semi-classically quantize the chiral soliton by the cranking method to see those effects on the matter solution. At present, soliton matter has been studied only at the classical energy level. In order to study the property of nucleon or Δ in medium, the spin and isospin of each of the soliton must be quantized. We hence perform the rotational collective quantization by the cranking formula and observe the saturation of nuclear and Δ matter. As shown in Sec. V, we obtained very shallow saturation.

Unfortunately, the study of the nuclear matter within the soliton model often fails to fit the experimental values, even in the saturation energy. This may be caused by the fact that the topological soliton picture is based on

*Electronic address: sawado@ph.noda.tus.ac.jp

†Electronic address: norikoshiiki@mail.goo.ne.jp

the approximation of large N_c -limit of QCD and therefore works well only in the very low energy scale. Thus our model improves slightly the situation in the sense that we take into account the quantum correction of $O(1/N_c)$ to the classical soliton mass of $O(N_c)$. However, it should be noted that as our model contains the valence quark explicitly, the physical meaning of such N_c counting is obscure. Of course, the prescription is still insufficient, and the obtained results will still room for improvement.

II. THE CHIRAL QUARK SOLITON MODEL

The CQSM was originally derived from the instanton liquid model of the QCD vacuum and incorporates the non-perturbative feature of the low-energy QCD, spontaneous chiral symmetry breaking. The vacuum functional is defined by [16]

$$\mathcal{Z} = \int \mathcal{D}\pi \mathcal{D}\psi \mathcal{D}\psi^\dagger \exp \left[i \int d^4x \bar{\psi} (i\cancel{\partial} - MU^{\gamma_5}) \psi \right] \quad (1)$$

where the SU(2) matrix

$$U^{\gamma_5} = \frac{1 + \gamma_5}{2} U + \frac{1 - \gamma_5}{2} U^\dagger \quad (2)$$

with

$$U = \exp(i\boldsymbol{\tau} \cdot \boldsymbol{\phi}/f_\pi) = \frac{1}{f_\pi}(\sigma + i\boldsymbol{\tau} \cdot \boldsymbol{\pi}) \quad (3)$$

describes chiral fields, ψ is quark fields and M is the dynamical quark mass. We choose the constituent quark mass $M = 420$ MeV which reproduces the experimental observables of the free nucleon correctly [19]. f_π is the pion decay constant and experimentally $f_\pi \sim 93$ MeV. Since our concern is the tree-level pions and one-loop quarks according to the Hartree mean field approach, the kinetic term of the pion fields which gives a contribution to higher loops can be neglected. Due to the interaction between the valence quarks and the Dirac sea, soliton solutions appear as bound states of quarks in the background of self-consistent mean chiral field. N_c valence quarks fill the each bound state to form a baryon. The baryon number is thus identified with the number of bound states filled by the valence quarks [24]. The $B = 1$ soliton solution has been studied in detail at classical and quantum level in [16, 17, 18, 19, 25].

The vacuum functional in Eq.(1) can be integrated over the quark fields to obtain the effective action

$$S_{\text{eff}}[U] = -iN_c \text{Lndet}(i\cancel{\partial} - MU^{\gamma_5}) \quad (4)$$

$$= -\frac{i}{2} N_c \text{Spln} D^\dagger D \quad (5)$$

where $iD = i\cancel{\partial} - MU^{\gamma_5}$ (iD is called the Dirac operator). This determinant is ultraviolet divergent and

must be regularized. Using the proper-time regularization scheme, we can write

$$\begin{aligned} S_{\text{eff}}^{\text{reg}}[U] &= \frac{i}{2} N_c \int_{1/\Lambda^2}^\infty \frac{d\tau}{\tau} \text{Sp} \left(e^{-D^\dagger D \tau} - e^{-D_0^\dagger D_0 \tau} \right) \\ &= \frac{iN_c T}{2} \int_{-\infty}^\infty \frac{d\omega}{2\pi} \int_{1/\Lambda^2}^\infty \frac{d\tau}{\tau} \text{Sp} \left[e^{-\tau(H^2 + \omega^2)} - e^{-\tau(H_0^2 + \omega^2)} \right] \end{aligned} \quad (6)$$

where T is the Euclidean time separation, Λ is a cut-off parameter evaluated by the condition that the derivative expansion of Eq.(4) reproduces the pion kinetic term with the correct coefficient *i.e.*

$$f_\pi^2 = \frac{N_c m^2}{4\pi^2} \int_{1/\Lambda^2}^\infty \frac{d\tau}{\tau} e^{-\tau M^2}, \quad (7)$$

and H is the Dirac one-quark Hamiltonian defined by

$$H = \frac{\boldsymbol{\alpha} \cdot \nabla}{i} + \beta M U^{\gamma_5}. \quad (8)$$

$D_0 \equiv D(U = 1)$ and $H_0 \equiv H(U = 1)$ correspond to the vacuum sectors. At $T \rightarrow \infty$, we have $e^{iS_{\text{eff}}} \sim e^{-iE_{\text{sea}}T}$. Integrating over ω in Eq.(6) and constructing a complete set of eigenstates of H with

$$H|\nu\rangle = \epsilon_\nu |\nu\rangle, \quad H_0|\nu\rangle^{(0)} = \epsilon_\nu^{(0)} |\nu\rangle^{(0)}, \quad (9)$$

one obtains the sea quark energy [18]

$$E_{\text{sea}}[U] = \frac{N_c}{4\sqrt{\pi}} \int_{1/\Lambda^2}^\infty \frac{d\tau}{\tau^{3/2}} \left(\sum_\nu e^{-\tau \epsilon_\nu^2} - \sum_\nu e^{-\tau \epsilon_\nu^{(0)2}} \right). \quad (10)$$

In the Hartree picture, the baryon states are the quarks occupying all negative Dirac sea and valence levels. Hence, if we define the total soliton energy E_{static} , the valence quark energy $E_{\text{val}}[U]$ should be added;

$$E_{\text{static}}[U] = N_c E_{\text{val}}[U] + E_{\text{sea}}[U]. \quad (11)$$

To obtain the $B = 1$ soliton solution, we impose the hedgehog ansatz on the chiral field

$$U(\mathbf{r}) = \exp(iF(r)\hat{\mathbf{r}} \cdot \boldsymbol{\tau}) = \cos F(r) + i\hat{\mathbf{r}} \cdot \boldsymbol{\tau} \sin F(r) \quad (12)$$

with the boundary conditions

$$F(0) = -\pi, \quad F(\infty) = 0. \quad (13)$$

The one-quark hamiltonian (8) reads

$$H(U^{\gamma_5}) = -i\boldsymbol{\alpha} \cdot \nabla + \beta M (\cos F(r) + i\gamma_5 \hat{\mathbf{r}} \cdot \boldsymbol{\tau} \sin F(r)). \quad (14)$$

This hamiltonian does not commute with the total angular momentum \mathbf{j} nor the isospin $\boldsymbol{\tau}/2$ but commute with the grand spin operator $\mathbf{K} = \mathbf{j} + \boldsymbol{\tau}/2$ with $[H, \mathbf{K}] = 0$. H

also commutes with the $\mathcal{P} = \gamma_0$ which turns to be a parity operator. As a result, the one-quark eigenstates are labeled by the $K = 0, 1, 2, \dots$ and the parity $\mathcal{P} = \pm$. The three valence quarks occupy the lowest states $K^{\mathcal{P}} = 0^+$ and are responsible for the baryon number ($= 1$) (non topological charge).

Field equations for the chiral fields can be obtained by demanding that the total energy in Eq.(11) be stationary with respect to variation of the profile function $F(r)$,

$$\frac{\delta}{\delta F(r)} E_{\text{static}} = 0 ,$$

which produces

$$S(r) \sin F(r) = P(r) \cos F(r), \quad (15)$$

where

$$S(r) = N_c \sum_{\nu} (n_{\nu} \theta(\epsilon_{\nu}) + \text{sign}(\epsilon_{\nu}) \mathcal{N}(\epsilon_{\nu})) \times \langle \nu | \gamma^0 \delta(|x| - r) | \nu \rangle, \quad (16)$$

$$P(r) = N_c \sum_{\nu} (n_{\nu} \theta(\epsilon_{\nu}) + \text{sign}(\epsilon_{\nu}) \mathcal{N}(\epsilon_{\nu})) \times \langle \nu | i \gamma^0 \gamma^5 \hat{\mathbf{r}} \cdot \boldsymbol{\tau} \delta(|x| - r) | \nu \rangle. \quad (17)$$

with

$$\mathcal{N}(\epsilon_{\nu}) = -\frac{1}{\sqrt{4\pi}} \Gamma\left(\frac{1}{2}, \left(\frac{\epsilon_{\nu}}{\Lambda}\right)^2\right)$$

and n_{ν} is the valence quark occupation number.

The procedure to obtain the self-consistent solution of Eq.(15) is that 1) solve the eigenequation in (9) under an assumed initial profile function $F_0(r)$, 2) use the resultant eigenfunctions and eigenvalues to calculate $S(r)$ and $P(r)$, 3) solve Eq.(15) to obtain a new profile function, 4) repeat 1) – 3) until the self-consistency is attained.

III. THE NUMERICAL BASIS

In this section we present the numerical method of eigen problem of the hamiltonian (14). The hamiltonian with hedgehog ansatz commutes with the parity and the grandspin operator given by

$$\mathbf{K} = \mathbf{j} + \boldsymbol{\tau}/2 = \mathbf{l} + \boldsymbol{\sigma}/2 + \boldsymbol{\tau}/2,$$

where \mathbf{j}, \mathbf{l} are respectively total angular momentum and orbital angular momentum. Accordingly, the angular basis can be written as

$$|(lj)KM\rangle = \sum_{j_3 \tau_3} C_{jj_3 \frac{1}{2} \tau_3}^{KM} \left(\sum_{m \sigma_3} C_{lm \frac{1}{2} \sigma_3}^{jj_3} |lm\rangle \left| \frac{1}{2} \sigma_3 \right\rangle \right) \left| \frac{1}{2} \tau_3 \right\rangle. \quad (18)$$

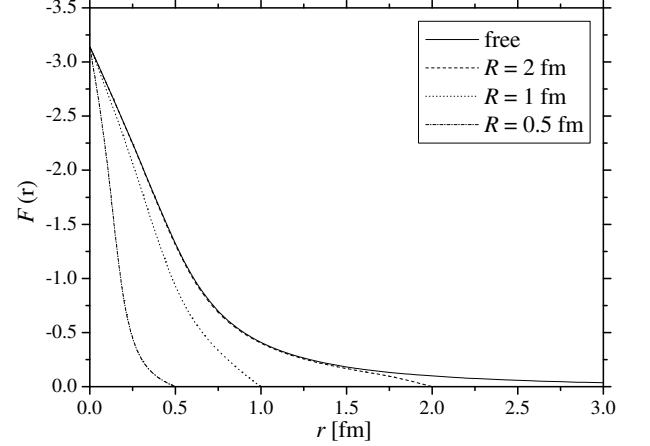


FIG. 1: Profile functions for $R = 0.5, 1, 2$ fm and the free soliton.

For $B = 1$ solution, following states are possible

$$\begin{aligned} |0\rangle &= |(K \ K + \frac{1}{2})KM\rangle, \\ |1\rangle &= |(K \ K - \frac{1}{2})KM\rangle, \\ |2\rangle &= |(K + 1K + \frac{1}{2})KM\rangle, \\ |3\rangle &= |(K - 1K - \frac{1}{2})KM\rangle. \end{aligned}$$

With this angular basis, the normalized eigenstates of the free hamiltonian in a spherical box with radius R can be constructed as follows:

$$\begin{aligned} u_{KM}^{(a)} &= N_k \begin{pmatrix} i\omega_{\epsilon_k}^+ j_K(kr) |0\rangle \\ \omega_{\epsilon_k}^- j_{K+1}(kr) |2\rangle \end{pmatrix}, \\ u_{KM}^{(b)} &= N_k \begin{pmatrix} i\omega_{\epsilon_k}^+ j_K(kr) |1\rangle \\ -\omega_{\epsilon_k}^- j_{K-1}(kr) |3\rangle \end{pmatrix}, \\ v_{KM}^{(a)} &= N_k \begin{pmatrix} i\omega_{\epsilon_k}^+ j_{K+1}(kr) |2\rangle \\ -\omega_{\epsilon_k}^- j_K(kr) |0\rangle \end{pmatrix}, \\ v_{KM}^{(b)} &= N_k \begin{pmatrix} i\omega_{\epsilon_k}^+ j_{K-1}(kr) |3\rangle \\ \omega_{\epsilon_k}^- j_K(kr) |1\rangle \end{pmatrix}, \end{aligned} \quad (19)$$

with

$$N_k = \left[\frac{1}{2} R^3 \left(j_{K+1}(kR) \right)^2 \right]^{-1/2} \quad (20)$$

and $\omega_{\epsilon_k > 0}^+, \omega_{\epsilon_k < 0}^- = \text{sgn}(\epsilon_k), \omega_{\epsilon_k > 0}^-, \omega_{\epsilon_k < 0}^+ = k/(\epsilon_k + M)$. The u and v correspond to the “natural” and “unnatural” components of the basis which stand for parity $(-1)^K$ and $(-1)^{K+1}$ respectively. The momenta are discretized by the boundary conditions $j_K(k_i R) = 0$. The orthogo-

TABLE I: The classical mass for the original Kahana-Ripka basis and modified version (in MeV), with $M = 400$ MeV, $R = 6$ fm. The error becomes of order $\sim 10^{-3}$.

	Valence	Vacuum	Total
free	191	637	1209
modified	192	633	1210

nality of the basis is then satisfied by

$$\begin{aligned}
 & \int_0^R dr r^2 j_K(k_i r) j_K(k_j r) \\
 &= \int_0^R dr r^2 j_{K\pm 1}(k_i r) j_{K\pm 1}(k_j r) \\
 &= \delta_{ij} \frac{R^3}{2} [j_{K\pm 1}(k_i R)]^2.
 \end{aligned} \quad (21)$$

Let us examine the boundary conditions for the chiral and Dirac fields to construct the nuclear matter solution in the Wigner-Seitz approximation. When the background chiral fields are periodic with lattice vector \mathbf{a} , the quark fields would be replaced by Bloch wave functions as $\psi(\mathbf{r} + \mathbf{a}) = e^{i\mathbf{k}\cdot\mathbf{a}}\psi(\mathbf{r})$. In the Wigner-Seitz approximation, however, the soliton is put on the center of the spherical unit cell with the radius R ($a = 2R$) and the dispersion \mathbf{k} is assumed to be zero. For the profile function $F(r)$, the periodicity and the unit topological charge inside the cell require the boundary conditions

$$\left. \begin{aligned} \sigma'(0) = \sigma'(R) = 0 \\ \pi(0) = \pi(R) = 0 \end{aligned} \right\} \Rightarrow F(0) = -\pi, F(R) = 0. \quad (22)$$

For the Dirac eigenstates, modification in the basis is needed. For odd number of K , the boundary condition is same as the free case with

$$j_K(k_i R) = 0. \quad (23)$$

For even K , the following conditions must be satisfied

$$\begin{aligned}
 j_{K+1}(k_i^{(a)} R) &= 0, \quad \text{for } u_{KM}^{(a)}, v_{KM}^{(a)}, \\
 j_{K-1}(k_i^{(b)} R) &= 0, \quad \text{for } u_{KM}^{(b)}, v_{KM}^{(b)}.
 \end{aligned} \quad (24)$$

Obviously the conditions (24) partially break the orthogonality of the basis (21) for the finite value of R . However we can solve the eigenvalue problem properly (see Table I). Although the motivation is different, the similar treatment has been already introduced in Ref.[26].

Fig. 1 shows the self-consistent profile functions for free ($R \rightarrow \infty$) and various values of the cell radius R . In Fig. 2, we present the results of the classical energy of the soliton and its valence and vacuum contributions as functions of R . We find the shallow minimum of the classical energy at $R \sim 1.2$ fm.

IV. SPURIOUS CENTER OF MASS CORRECTION

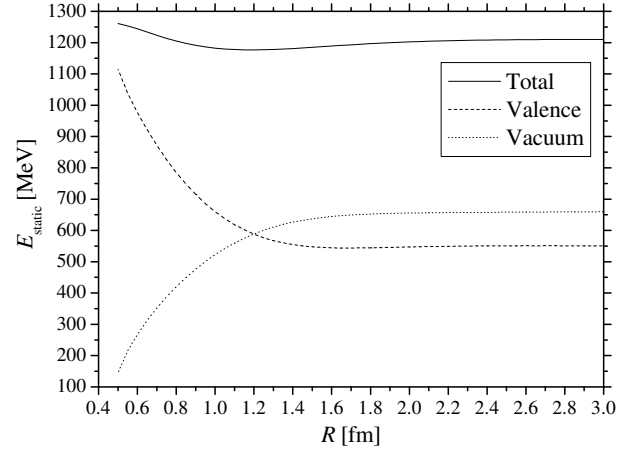


FIG. 2: Classical soliton energy and its valence and vacuum contributions (11).

The minimum found in Fig. 2 is not regarded as a true saturation point because it contains the zero-point energy contributions. The quark contribution to the mean-field expectation value of the square of the total momentum \mathbf{P}^2 appears at the classical level although it should be zero because the soliton is rest at the cell center in the present approximation. Therefore, the corresponding kinetic energy should be subtracted from the total energy. The effects of the spurious center of mass motion is roughly estimated by the method of Pobylitsa *et al.* [27]. Considering the translational degrees of freedom and performing their quantization, one obtains the correction at a rest frame as

$$E_{\text{static}} \rightarrow \tilde{E}_{\text{static}} = E_{\text{static}} - \frac{\langle \mathbf{P}^2 \rangle}{2E_{\text{static}}}. \quad (25)$$

The correction is easily evaluated by using the numerical basis given in Eq. (19) as $\mathbf{P}^2 u_{KM}^{(a)}(k_i r) = k_i^2 u_{KM}^{(a)}(k_i r)$. As is shown in Fig. 3, the minimum disappears after removing the zero-point energy contributions (25). This is explained by the observation that the contribution of the center of mass motion becomes small with increasing density (see Fig. 4 and the caption).

V. COLLECTIVE QUANTIZATION

The solitons that we have obtained in the previous section are classical objects and therefore must be quantized to assign definite spin and isospin to them. For the solitons in the free space, quantization can be performed semiclassically for their rotational zero modes. For the hedgehog soliton, because of its topological structure, a rotation in isospin space is followed by a simultaneous spatial rotation. Let us introduce the dynamically ro-

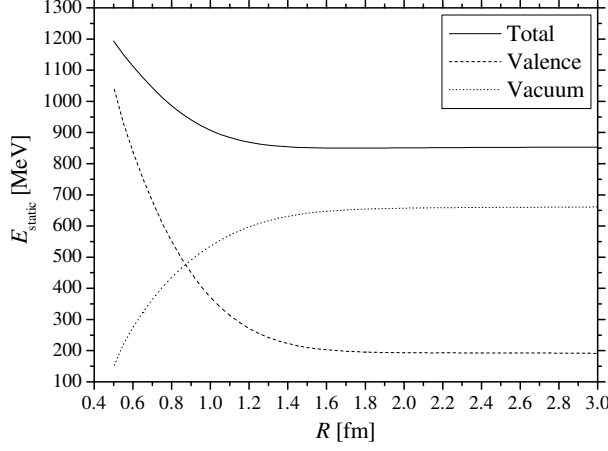


FIG. 3: Classical soliton energy after removing the spurious center of mass motion (25).

tated chiral fields

$$\tilde{U}(\mathbf{x}, t) = A(t)U(\mathbf{x})A(t)^\dagger, \quad A(t) \in \text{SU}(2)_I. \quad (26)$$

In a crystal configuration, the solitons are fixed on the spatial lattice point and their isospin orientation is chosen so as to minimize the energy of the system. If one rotates each soliton in the crystal, it changes the isospin orientation and increases the energy. Thus there is only one isospin collective coordinate corresponding to the overall orientation of the crystal in isospace, called global isospin, in the soliton crystal [1, 28].

The Wigner-Seitz treatment with spherical cell approximation may cure the situation. Because in this approximation the information of the crystalline structure, hence, the isospin structure is completely lost at least in the low-density, the rotational zero-mode would be recovered. Thus, we apply the zero-mode quantization method to the WS-cell to estimate the nucleon and the delta mass splitting in the matter.

By transforming the rotating frame of reference, the Dirac operator with Eq. (26) can be written as

$$i\tilde{D} = A(t)\gamma^0[i\partial_t - H(U^{\gamma^5}) + \Omega]A(t)^\dagger \quad (27)$$

where

$$\Omega = iA^\dagger \dot{A} = \frac{1}{2}\Omega^a \tau_a. \quad (28)$$

Ω is the angular velocity operators for an isorotation. Assuming that the rotation of the soliton is adiabatic, we shall expand the effective action S_{eff} around the classical solution $U(\mathbf{x})$ with respect to the angular momentum velocity Ω up to second order [29]

$$S_{\text{eff}}(\tilde{U}) = S_{\text{eff}}(U) - iN_c \text{Sp} [\log(i\partial_t - H + \Omega)] - \text{Sp} [\log(i\partial_t - H)].$$

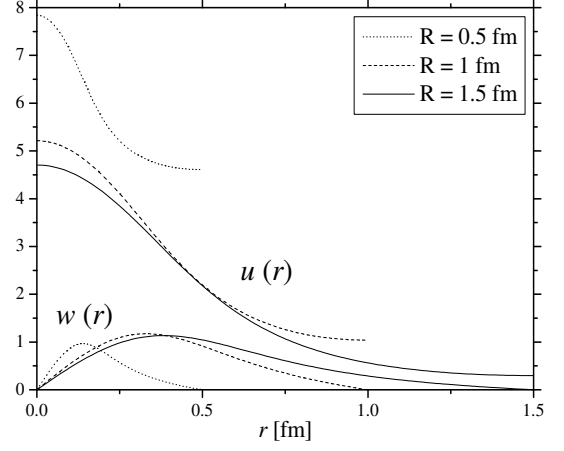


FIG. 4: The “upper” $u(r)$ and the “lower” $w(r)$ component of valence quark wave functions for various cell radius R with the boundary condition $w(R) = 0$. Non vanishing values of upper component at the cell boundary $u(R)$ come from the zero-mode elements in the basis.

With the proper-time regularization, we have

$$S_{\text{eff}}^{\text{reg}}(\tilde{U}) = S_{\text{eff}}^{\text{reg}}(U) + \frac{1}{2} \sum_{ab} \int dt [I_{\text{sea},ab} \Omega^a(t) \Omega^b(t)]$$

where $I_{\text{sea},ab}$ is the vacuum sea contribution to the moments of inertia defined by

$$I_{\text{sea},ab} = \frac{1}{8} N_c \sum_{\nu, \mu} f(\epsilon_\mu, \epsilon_\nu, \Lambda) \langle \nu | \tau_a | \mu \rangle \langle \mu | \tau_b | \nu \rangle, \quad (29)$$

with the cutoff function $f(\epsilon_\mu, \epsilon_\nu, \Lambda)$

$$f(\epsilon_\mu, \epsilon_\nu, \Lambda) = -\frac{2\Lambda}{\sqrt{\pi}} \frac{e^{-\epsilon_\mu^2/\Lambda^2} - e^{-\epsilon_\nu^2/\Lambda^2}}{\epsilon_\mu^2 - \epsilon_\nu^2} + \frac{\text{sgn}(\epsilon_\mu) \text{erfc}(|\epsilon_\mu|/\Lambda) - \text{sgn}(\epsilon_\nu) \text{erfc}(|\epsilon_\nu|/\Lambda)}{\epsilon_\mu - \epsilon_\nu}.$$

Similarly, for the valence quark contribution we have

$$I_{\text{val},ab} = \frac{1}{2} N_c \sum_{\mu \neq \text{val}} \frac{\langle \text{val} | \tau_a | \mu \rangle \langle \mu | \tau_b | \text{val} \rangle}{E_\mu - E_{\text{val}}}. \quad (30)$$

The total moments of inertia are then given by the sum of the vacuum and valence, $I_{ab} = I_{\text{val},ab} + I_{\text{sea},ab}$. The hedgehog ansatz of the chiral fields ensure the relation for the moment of inertia

$$I_{11} = I_{22} = I_{33}. \quad (31)$$

The quantization condition for the collective coordinate, $A(t)$, define a body-fixed isospin operator \mathbf{K} as

$$I_{ab} \Omega^b \rightarrow -\text{tr} \left(A \frac{\tau_a}{2} \frac{\partial}{\partial A} \right) \equiv -k_a, \quad (32)$$

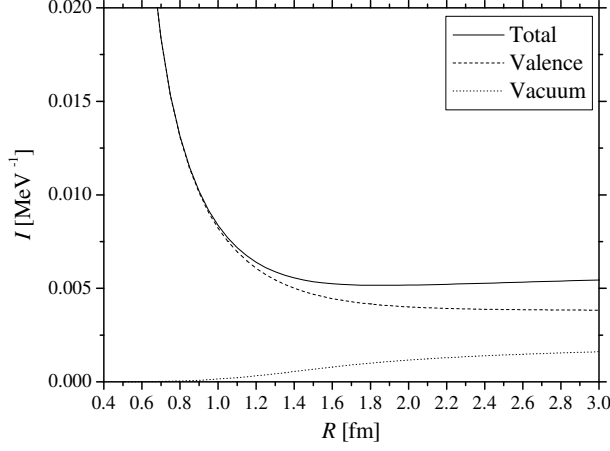


FIG. 5: Moment of inertia : the vacuum (29) and the valence (30) contribution and their sum.

These are related to the usual coordinate-fixed isospin operator i_a by transformation,

$$i_a = -\frac{1}{2} \text{Tr}[\tau_a A(t) \tau^b A(t)^\dagger] k_b. \quad (33)$$

To estimate the quantum energy corrections, let us introduce the basis functions of the spin and isospin operators which were inspired from the cranking method for nuclei [31],

$$\langle A | i i_3 k_3 \rangle = \sqrt{\frac{2i+1}{8\pi^2}} (-1)^{i+i_3} D_{-i_3 k_3}^i(A)$$

where D is the Wigner rotation matrix. Finally, we find the quantized energies of the soliton as

$$E = E_{\text{static}} + \frac{i(i+1)}{2I_{33}} \quad (34)$$

where $i(i+1)$ is eigenvalues of the Casimir operator \mathbf{i}^2 . The moment of inertia for the vacuum (29) and valence (30) and their sum are given in Fig. 5. In Fig. 6, we present the energy of nucleon ($i = \frac{1}{2}$) and Δ ($i = \frac{3}{2}$).

In this cranking procedure, the zero-point energy of the rotational motion $\langle \mathbf{i}^2 \rangle / 2I_{33}$ must be removed from Eq. (34) [27, 30]. Finally, we obtain the mass of nucleon and delta

$$E_N = \tilde{E}_{\text{static}} - \frac{3}{4I_{33}}, \quad (35)$$

$$E_\Delta = \tilde{E}_{\text{static}} + \frac{3}{4I_{33}}. \quad (36)$$

Fig. 7 shows the energy of nucleon and delta after subtracting the spurious zero-point energy. The minimum for nucleon is observed at $R \sim 1.8$ fm which corresponds to the density $\rho_N \sim 0.04 \text{ fm}^{-3}$. This value is much

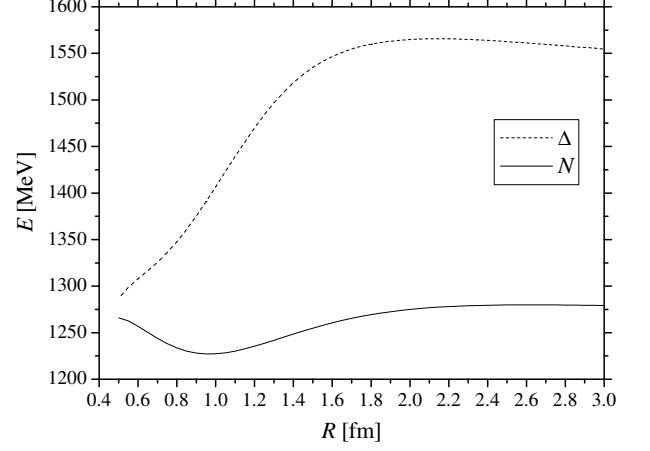


FIG. 6: Quantized soliton energies of nucleon N and delta resonance $\Delta(1232)$ (34).

lower than the experimental value. The binding energy is $E_B \sim 18$ MeV which is not far from the experimental observation. For Δ , we also find the shallow minima at $R \sim 1.22$ fm which corresponds to $\rho_\Delta \sim 0.13 \text{ fm}^{-3}$. The Δ saturation is attained at the density $\rho_\Delta / \rho_N \sim 3.2$ which is close to the prediction of density $\rho_\Delta / \rho_N \sim 2-3$ in the framework of the quantum hadrodynamics [32, 33]. The advantage of our approach is that the model does not require any tuning parameter for the Δ spectra in the hadrodynamics calculations.

VI. SUMMARY

We have studied soliton solutions in nuclear medium by using the Wigner-Seitz approximation. The chiral quark soliton model was used to obtain the classical soliton solution. In this letter we especially focused on the properties of nucleon and Δ in matter. We quantized the soliton semiclassically. The adiabatic rotation for the (iso-)rotational zero mode was performed and the nuclear saturation points were obtained for nucleon and Δ matter.

Here we did not consider the following effects which should be investigated to develop our understanding of the dense nuclear matter:

- band structure of the quarks
- R dependence of the constituent quark mass M and the cutoff parameter for the vacuum Λ
- inclusion of the heavier mesons (ρ, ω, \dots) to the soliton solutions
- improvement of the correction by the zero point energy and Casimir effects

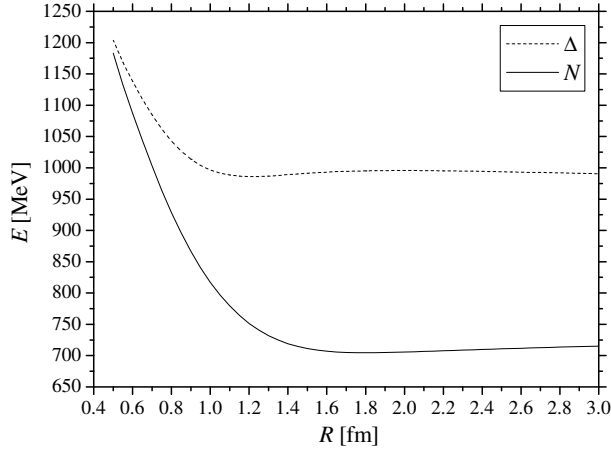


FIG. 7: Masses of N, Δ , after spurious energy subtractions (35)-(36).

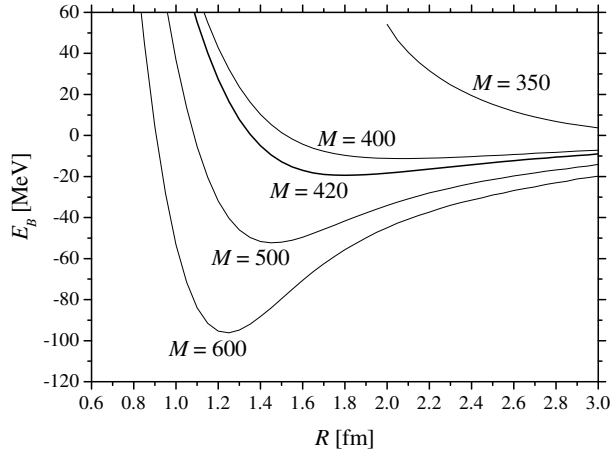


FIG. 8: Binding energy of nucleon for the various constituent quark mass M (in MeV).

- quark-meson couplings and the Fermi motion of the baryons
- crystalline order in high density phase
- $SU(3)$ extension.

As is expected, our model provides much lower value of the saturation density than the experiment. In this analysis, the Wigner-Seitz cell is approximated by a sphere and thus high density matter is attained by shrinking the cell volume with the spherical shape of each soliton unchanged. However, in reality, the neighborhood solitons start to overlap and the structure will be deformed from uniform nuclear matter at high density. In this phase, the hedgehog ansatz should not be appropriate any more.

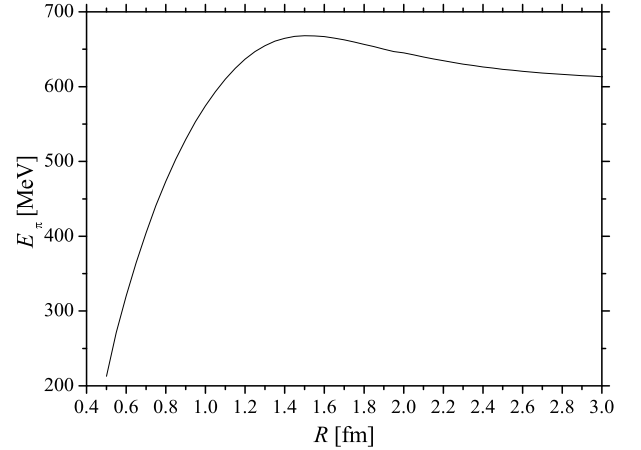


FIG. 9: Kinetic energy of the pion (37).

We observed the increase in the zero mode of the center of mass motion of the soliton for higher density, which means that the soliton tends to rest in the WS approximation. In this case, we should employ the exact WS cell which reflects the background crystal symmetry instead of sphere, to get higher saturation density. The inclusion of band effects may also improve our results. In Ref. [14], the authors imposed the Bloch-like boundary conditions on the s-wave valence quark wave function and estimated the soliton energy self-consistently. They found that the effects of the admixtures of higher states are small except for the scalar quark density. In fact, the band structure will appear at some critical density and the correction for the quantum energy may become more important at the dense medium because the radius of the soliton, that is, the moment of inertia, strongly depend on the position of the band [22].

Generally speaking, the constituent quark mass M is momentum- and density-dependent [16]. We chose the value $M = 420$ MeV as it reproduces the free nucleon observable. In Fig. 8, one can see that for larger value of M , the saturation point goes to inward and the binding becomes deeper. Varying the value of M for each density may give a better result for the saturation point.

An important feature of the nucleon in a matter is about its size. It is believed that the nucleon will swell in the medium. The authors of Ref. [34] observe such effect with reducing effective quark mass M^* in the Nambu-Jona-Lasinio type quark-soliton model. We confirmed within our model that as smaller the M , the size of the soliton increases. But in that case, the saturation becomes shallower (Fig. 8). Recently, we investigated soliton solutions in the CQSM taking into account ρ, ω mesons which will improve the short distance physics. We are able to obtain deeper binding energy as decreasing the value of M . We will report it on forthcoming article.

In Fig. 6, one finds that the spectra of nucleon and

Δ are too small compared to the experimental values. Obviously it is due to the subtraction of the zero-point corrections. A little more sophisticated approach of the spurious motion is performed in Ref. [14] and by applying this approach to our analysis, the results will be improved to a certain extent. Also, the meson coupling to the quark inside nucleon and Δ should be important to shift the minima at higher density.

In Fig. 6 and Fig. 7, one finds the nucleon- Δ mass difference gradually decreases as matter density increases and eventually it vanishes. The reduction in the mass difference has been observed previously in a similar chiral soliton model but employing somewhat different projection technique for quantum number [35, 36]. In the present formulation, the behavior is not fully understood because it should be explained by the dynamics of hadrons, that is, QCD. In the naive $SU(6)$ quark model, the mass difference is ascribed to the hyperfine splitting [37]. The reduction may imply the increase of the distance between quarks. In fact, in Fig. 4, one can see the concentration of the quarks at the cell boundary as the density increases.

Alternatively, if we understand the Δ as a composite object (resonance state) of the nucleon and pion, the mass difference can be interpreted as the energy of pions bound to the nucleon. Although it is absent in the

present formulation, the pion kinetic energy inside the soliton can be estimated as

$$E_\pi = \frac{f_\pi^2}{4} \int d^3x \text{tr} \partial_k U^\dagger \partial_k U \\ = 2\pi f_\pi^2 \int_0^R r^2 dr \left(F'(r)^2 + \frac{\sin^2 F(r)}{r^2} \right). \quad (37)$$

In Ref. [22], the authors introduced the r - and the cutoff parameter of the vacuum Λ -dependent form of the pion decay constant $f_\pi(r, \Lambda)$ and estimated its density dependence with the Λ whose value is set for the free space value of f_π . The $f_\pi(r, \Lambda)$ determined in such a way is essentially valid only for the free space limit $R \rightarrow \infty$. Therefore we shall simply take the value in free space $f_\pi = 93$ MeV. Fig. 9 shows the result of the kinetic energy of pions as a function of R and one can observe that the energy is reduced as the density increases. This reduction of the pion kinetic energy may contribute to the reduction of the mass difference.

Our formulation is directly applicable to the $SU(3)$ octet-decuplet baryon spectra in nuclear matter [26, 38]. After the above effects are properly incorporated and more realistic estimation of the saturation points is achieved, it will be interesting to study the $SU(3)$.

-
- [1] Igor Klebanov, Nucl. Phys. B **262**, 133 (1985).
 - [2] E. Wüst, B. E. Brown and A. D. Jackson, Nucl. Phys. A **468**, 450 (1987).
 - [3] Alfred S. Goldhaber and N. S. Manton, Phys. Lett. B **19**, 231 (1987).
 - [4] L. Castillejo, P. S. Jones, A. D. Jackson, J. J. M. Verbaarschot and A. Jackson, Nucl. Phys. A **501**, 450 (1987).
 - [5] M. Kugler and S. Shtrikman, Phys. Rev. D **40**, 3421 (1989).
 - [6] Byung-Yoon Park, Dong-Pil Min, Mannque Rho and Vincente Vento, Nucl. Phys. A **707**, 381 (2002).
 - [7] Joachim Achtezhnter, Werner Scheid and Lawrence Wilets, Phys. Rev. D **32**, 2414 (1985).
 - [8] B. Banerjee, N. K. Glendenning and V. Soni, Phys. Lett. B **155**, 213 (1985).
 - [9] N. K. Glendenning and B. Banerjee, Phys. Rev. C **34**, 1072 (1986).
 - [10] Detlev Hahn and Norman K. Glendenning, Phys. Rev. C **36**, 1181 (1987).
 - [11] Urban Weber and Judith A. McGovern, Phys. Rev. C **57**, 3376 (1998).
 - [12] H. Reinhardt, B. V. Dang, and H. Schulz, Phys. Lett. B **159**, 161 (1985).
 - [13] M. C. Birse, J. J. Rehr and L. Wilets, Phys. Rev. C **38**, 359 (1988).
 - [14] Nir Barnea, Timothy S. Walhout, Nucl. Phys. A **677**, 367 (2000).
 - [15] M. Kutschera, C. J. Pethick and D. G. Ravenhall, Phys. Rev. Lett. **53**, 1041 (1984).
 - [16] D. I. Diakonov, V. Yu. Petrov, and P. V. Pobylitsa, Nucl. Phys. B **306**, 809 (1988).
 - [17] H. Reinhardt and R. Wünsch, Phys. Lett. B **215**, 577 (1988).
 - [18] Th. Meissner, F. Grümmer, and K. Goeke, Phys. Lett. B **227**, 296 (1989).
 - [19] For detailed reviews of the model see: R. Alkofer, H. Reinhardt and H. Weigel, Phys. Rept. **265**, 139 (1996); Chr. V. Christov, A. Blotz, H.-C. Kim, P. Pobylitsa, T. Watabe, Th. Meissner, E. Ruiz Arriola, K. Goeke, Prog. Part. Nucl. Phys. **37**, 91 (1996).
 - [20] D. Diakonov, V. Petrov and M. Polyakov, Z. Phys. A **359**, 305 (1997).
 - [21] T. Nakano *et al.*, Phys. Rev. Lett. **91**, 012002 (2003).
 - [22] P. Amore and A. De Pace, Phys. Rev. C **61**, 055201 (2000).
 - [23] I. Adjali, I. J. Aitchison, and J. A. Zuk, Nucl. Phys. A **537**, 457 (1992).
 - [24] S. Kahana and G. Ripka, Nucl. Phys. A **429**, 462 (1984).
 - [25] M. Wakamatsu and H. Yoshiki, Nucl. Phys. A **524**, 561 (1991).
 - [26] H. Weigel, R. Alkofer and H. Reinhardt, Nucl. Phys. B **387**, 638 (1992).
 - [27] P. V. Pobylitsa, E. Ruiz Arriola, Th. Meissner, F. Grümmer, K. Goeke and W. Broniowski, J. Phys. G **18**, 1455 (1992).
 - [28] W.K. Baskerville, Phys. Lett. B **380**, 106 (1996).
 - [29] L. C. Biedenharn, Y. Dothan and M. Tarlini, Phys. Rev. D **31**, 649 (1985).
 - [30] Thomas D. Cohen and Wojciech Broniowski, Phys. Rev. D **34**, 3472 (1986).
 - [31] A. Bohr and B. Mottelson, *Nuclear structure, Vol. II*

- (World Scientific Publishing Co. Pte. Ltd, Singapore, 1998).
- [32] B. M. Waldhauser, J. Theis, J. A. Maruhn, H. Stöcker, and W. Greiner, Phys. Rev. C **36**, 1019 (1987).
 - [33] Zhuxia Li, Guangjun Mao, Yizhong Zhuo, and Walter Greiner, Phys. Rev. C **56**, 1570 (1997).
 - [34] Chr.V.Christov, K.Goeke, Nucl. Phys. A **564**, 551 (1993).
 - [35] E.Ruiz Arriola, Chr.V.Christov and K. Goeke, Phys. Lett. B **225**, 22 (1989).
 - [36] Chr.V.Christov, M. Fiolhais, E.Ruiz Arriola and K. Goeke, Phys. Lett. B **243**, 333 (1990).
 - [37] A. De Rujula, H. Georgi and S. L. Glashow, Phys. Rev. D **75**, 147 (1975).
 - [38] A. Blotz, D. Diakonov, K. Goeke, N. W. Park, V. Petrov and P. V. Pobylitsa, Nucl. Phys. A **555**, 765 (1993).